Earthquake Geotechnical Engineering for Protection and Development of Environment and Constructions – Silvestri & Moraci (Eds)
© 2019 Associazione Geotecnica Italiana, Rome, Italy, ISBN 978-0-367-14328-2

Development of fragility curves for underground box tunnels from nonlinear frame analysis

D. Park
Department of Civil and Environmental Engineering, Hanyang University, Seoul, Korea

T.H. Lee & D.D. Nguyen
Department of Civil Engineering, Konkuk University, Seoul, Korea

J.K. Ahn
Korea Meteorological Administration, Seoul, Korea

ABSTRACT: We develop seismic fragility curves ofa double box tunnel for three damage states from nonlinear frame analyses. A suite of site profiles is used to evaluate the effect of soil characteristics on the calculated fragility curve. We use two ground motion intensity measures, which are peak ground acceleration (PGA) and the ratio of the peak ground velocity to the average shear wave velocity within 30m from the surface (PGV/V_{s30}). The fragility curve is demonstrated to be highly dependent on the site profile. The influence of the site effects on the fragility curve is reduced when PGV/V_{s30} is used. This is because both the intensity of the ground motion and the soil stiffness is accounted for in the parameter PGV/V_{s30}. It is therefore recommended that PGV/V_{s30} be used instead of PGA to generate fragility curves for underground structures.

1 INTRODUCTION

Even though underground structures are considered less vulnerable to seismic excitations compared with above-ground structures, significant destructions of tunnels were observed during previous earthquake events (Downding & Rozan 1978; Hashash et al. 2001, Iida et al. 1996). These damages have raised a need to assess the seismic vulnerability of existing underground structures. For that, the fragility curve is a useful tool to predict the probability of damage of structures at a given level of seismic intensity measure.

Fragility curves of tunnels can be developed by using either empirical or numerical approaches. The American Lifelines Alliance (ALA 2001) proposed empirical fragility curves for mountain and cut-and-cover tunnels with respect to the peak ground acceleration (PGA). HAZUS (2004) also presented a set of empirical fragility curves for bored and cut-and-cover tunnels with respect to PGA and the permanent ground displacement based on the field observation data. Due to limitations of observed damage data from earthquake events, the numerical simulation is a preferable method for deriving fragility curves of tunnels. Argyroudis & Pitilakis (2012) developed a set of fragility curves for a shallow circular and cut-and-cover tunnels with respect to PGA. Argyroudis et al. (2017) generated fragility curves for two circular shallow tunnels considering the effect of corrosion of the tunnel lining. Liu et al. (2016) performed the incremental dynamic analysis to deriving fragility curves for Daikai subway station with respect to the peak ground velocity (PGV). Recently, seismic fragility curves for a group of circular tunnels using spectra acceleration were proposed in Qiu et al. (2018). The previous studies mostly considered a specific site and an earthquake intensity measure in fragility curves.

The purpose of this study is to develop fragility curves for a double box metro tunnel in various site profiles using PGA at the ground surface and PGV/V_{s30} as seismic intensity

measures. V_{s30} is the average shear wave velocity within 30 m of the site profile depth. Three damage states, proposed by Lee et al. (2016) based on nonlinear frame analysis, were used to construct fragility curves. The effect of used intensity measures and site profiles on fragility curves were assessed.

2 TUNNEL CONFIGURATION AND SITE PROFILES

The investigated structure is a double box cut-and-cover tunnel which was built for subway in South Korea. The height and width of the tunnel are 7 m and 13 m, respectively. The thickness of the outer frame is 1.0 m, while the center column dimension is 0.4 x 1.0 m, as shown in Figure 1.

Sixteen site profiles classified into site class B, C, and D were selected for analyses, in which four profile depths are included 30, 50, 100, and 150 m. Figure 2 shows the site profiles in terms of the shear wave velocity (V_s).

3 PROCEDURE FOR DEVELOPING FRAGILITY CURVES

Numerous studies pointed out that the difference between a pseudo-static and dynamic analysis was insignificant (Hwang & Lu 2007, Hashash et al. 2010, Argyroudis & Pitilakis 2012). Also, the pseudo-static approach has been commonly used in both practical design (MLTM 2009, Iai 2005, Wang 1993, Wood 2004) and research (Anderson 2008, Argyroudis et al. 2013, Argyroudis et al. 2017, Park et al. 2009, Tsinidis et al. 2016, Debiasi et al. 2013, Yoo et al. 2017, Zou et al. 2017). Therefore, a series of pseudo-static analyses were performed to derive fragility curves of the tunnel in this study. The procedure for developing fragility curves of tunnels is briefly described as follows.

- Step 1. Perform 1D site response equivalent linear analysis for a suite of ground motions.
- Step 2. Build up the soil-tunnel system using the soil spring nonlinear frame model.
- Step 3. Impose the soil displacement from Step 1 on the structural model.
- Step 4. Obtain bending moment at the critical section of tunnel lining
- Step 5. Define damage state based on damage index (DI), which is expressed as the ratio of the bending moment (M) to the yield moment (My) of the critical section of the tunnel.
- Step 6. Develop the relationship between DI (M/My) and seismic intensity measures.

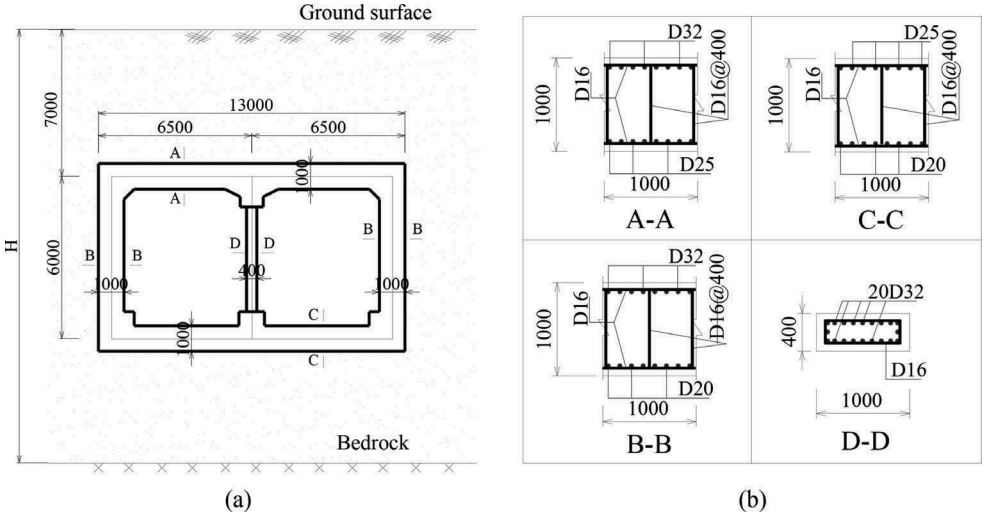

Figure 1. Tunnel cross section (a) and reinforcement detail of tunnel lining (b)

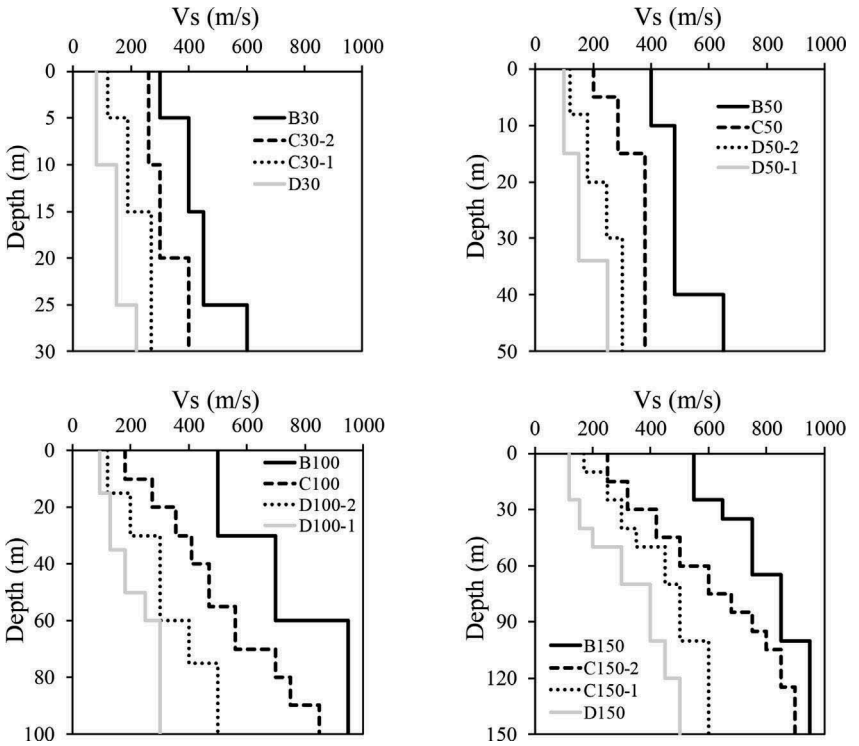

Figure 2. Selected site profiles

- Step 7. Calculate mean and standard deviation for each damage state using regression.
- Step 8. Generate fragility curves based on mean and standard deviation parameters.

4 1D SITE RESPONSE ANALYSIS AND STRUCTURAL MODELING

The horizontal displacements of sixteen selected site profiles were calculated by the 1D equivalent linear site response analysis using Deepsoil v6.0 (Hashash et al. 2015). The sand soil type was assumed for all site profiles and the model of Darendeli (Darendeli 2001) was used. The over-consolidation ratio was set to 1.0, the horizontal at-rest earth pressure factor was 0.5, plasticity index was zero, and the number of cycles of loading and the excitation frequency were defined as 10 and 1.0, respectively. The input motions were imposed as rock outcrop motions. Figure 3 illustrates the peak horizontal displacements of site profiles under different ground motion records.

The racking behavior is the dominant response of rectangular tunnels under a seismic loading. The double box tunnel was modeled using frame elements available in SAP2000 (CSI 2011). We performed the mesh convergence analysis to determine the mesh size, which concluded that 64 elements were required per a structural frame member. One dimensional nonlinear material models were applied for both concrete and reinforcing bar of the tunnel linings whose details can be found in Lee et al. (2016). A series of soil springs in the normal and the shear directions were attached to all nodes to account for the soil resistance. The spring constants were calculated according to the seismic design code for metropolitan subway of Korea (MLTM 2009). The horizontal (K_H) and vertical (K_V) normal spring constants were defined as

$$K_H = k_{h0}\left(\frac{h}{30}\right)^{-3/4} \tag{1}$$

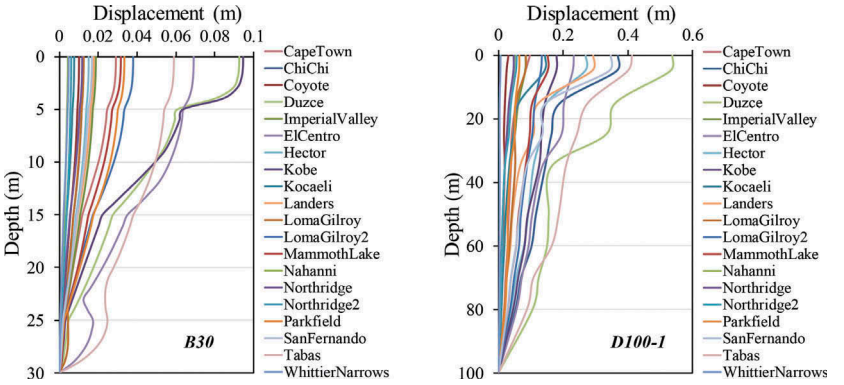

Figure 3. Peak displacement of site profiles

$$K_V = k_{h0}\left(\frac{b}{30}\right)^{-3/4} \tag{2}$$

where $K_{h0} = (1/30)E_D$, h and b are the height and the width of the tunnel, respectively, E_D is elastic modulus of the surrounding soil. The shear springs for vertical (K_{SS}) and horizontal (K_{SB}) frames were defined as

$$K_{SS} = \frac{1}{4}K_H \tag{3}$$

$$K_{SB} = \frac{1}{4}K_V \tag{4}$$

We also developed the relationship between racking (R) and flexibility ratio (F) of this study and compared with the published results (Andeson 2008, Penzien 2000, Wang 1993). This comparison was presented in Nguyen et al. (2018), showing a good agreement. The pseudo-static analysis procedure presented by Iai (2005) was adopted in this study. Figure 4 depicts the boundary conditions and imposed loads on the tunnel.

5 DAMAGE STATES AND FRAGILITY CURVES

The bending moment of the tunnel was calculated by applying the soil displacement on the tunnel-soil model. We observed that the top-right and bottom-left corners of the tunnel frame are the critical sections. The damage states were developed based on nonlinear pushover analyses. The damage index (DI) was defined in terms of the ratio of the moment demand (M) to the yield moment (My) of the critical section and number of plastic hinges formed in the tunnel frame. A detailed simulation and results were presented in Lee et al. (2016). Table 1 shows the damage states and the corresponding DIs adopted in this study.

The engineering demand parameter (EDP) used in this study is the ratio of the moment demand (M) to the yield moment (My) at the critical section of tunnel lining. Figure 5 plots the natural logarithm of DI against PGV/V_{s30} for two selected sites. It is shown that DI is strongly correlated to PGV/V_{s30}.

A fragility function expresses the conditional probability that a structure reaches or exceeds a damage state when subjected to a given level of ground motion intensity. In this paper, the fragility function is assumed as a log-normal cumulative distribution function, expressed by

$$P[DS|IM] = \Phi\left[\frac{\ln(IM) - \mu}{\beta}\right] \tag{5}$$

where P[DS|IM] is the probability of exceeding the damage state (DS) at a given ground motion intensity measure (IM): PGA or PGV/V_{s30}.Φ[-] is standard normal cumulative

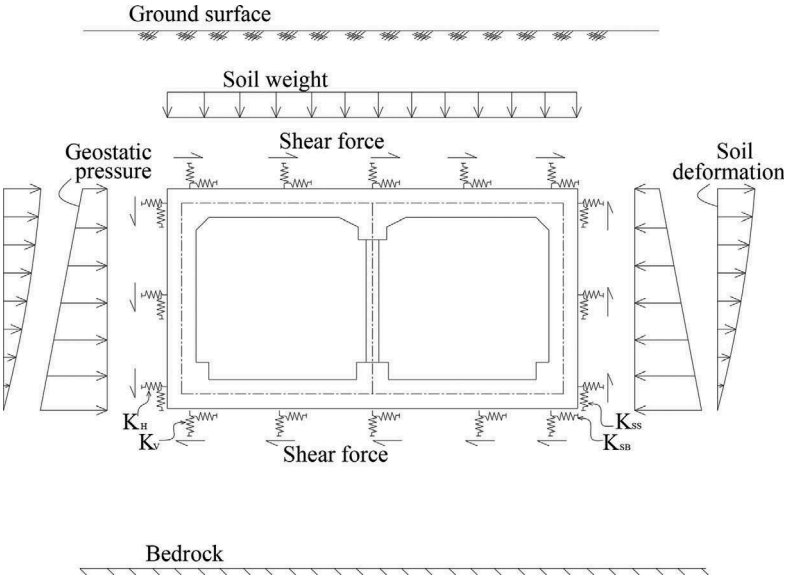

Figure 4. Boundary condition and applied loads to the tunnel

Table 1. Damage states and corresponding damage indices (Lee et al. 2016)

Damage state	Damage index (DI, M/My)
None	DI < 1.0
Minor/Slight	1.0 ≤ DI < 1.2
Moderate	1.2 ≤ DI < 2.0
Extensive	2.0 ≤ DI

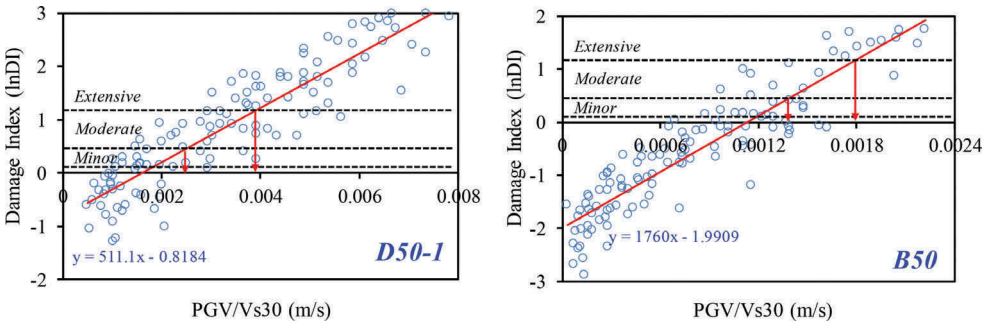

Figure 5. DI and seismic intensity measure and estimation of mean values for damage states

distribution function. μ and β are the median and standard deviation of $ln(IM)$, respectively. The total standard deviation β is calculated by combining of two uncertainties, the capacity of tunnel (β_C) and the ground motion demand (β_D), expressed by

$$\beta = \sqrt{\beta_C^2 + \beta_D^2} \tag{6}$$

The capacity uncertainty (μ_C) is set to 0.3 (Salmon et al. 2003). The demand uncertainty due to earthquakes (μ_D) is calculated by the average standard deviation of the damage indices in

the linear regression analysis (Ang & Tang 2007). The uncertainty due to the definition of damage states was neglected in this study.

Figure 6 shows the fragility curves of the tunnel for three damage states in various site profiles. The solid curves represent the mean fragility curves of site classes. It was found that the seismic vulnerability decreases with an increment of the soil stiffness, because a stiffer soil yields a smaller displacement that produces smaller internal forces in the tunnel lining.

Figure 7 shows fragility curves of the tunnel for all site profiles using PGV/V_{s30}, which is an intensity measure widely used to approximate the free-field shear strain. $PGV/V_{s30}$is used because both the intensity of the ground motion and the soil stiffness is accounted for in the parameter.

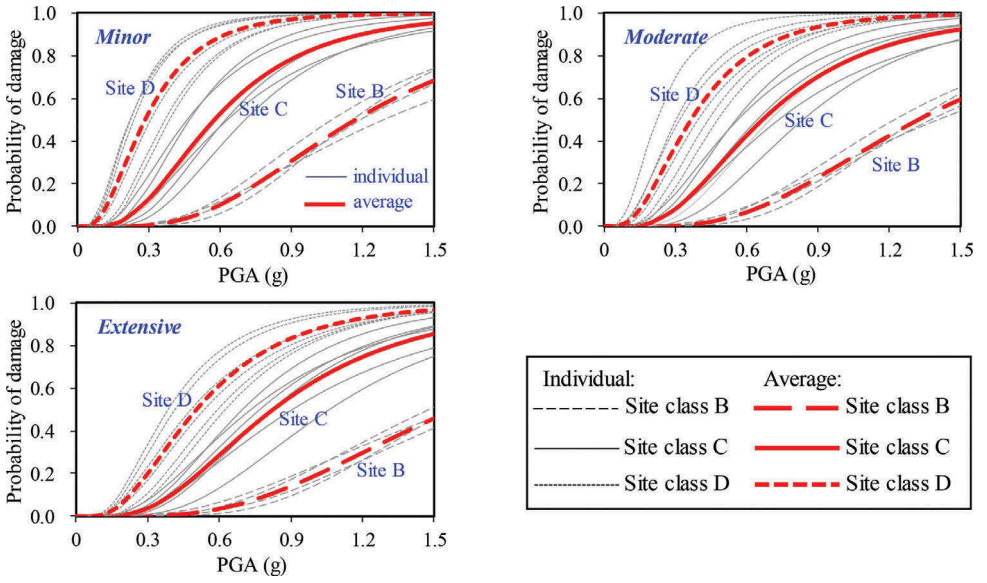

Figure 6. Fragility curves of the double box tunnel using PGA

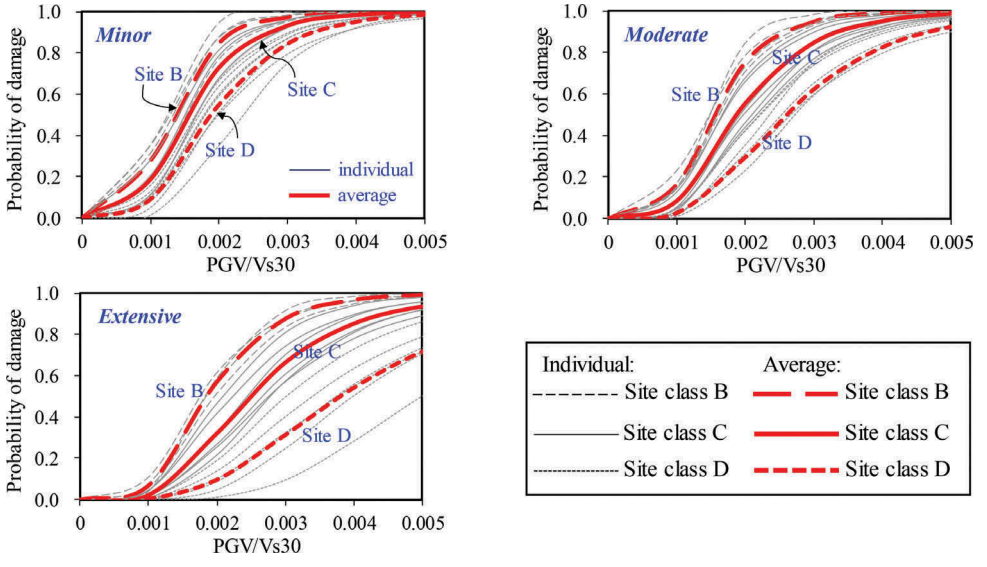

Figure 7. Fragility curves of the double box tunnel using PGV/Vs30

Table 2. Fragility function parameters of the double box tunnel

Site class	Damage state	PGA surface		PGV/V_{s30}	
		μ (g)	β	μ	β
B	Minor	1.18	0.61	0.130%	0.51
	Moderate	1.33	0.61	0.151%	0.51
	Extensive	1.58	0.61	0.186%	0.51
C	Minor	0.58	0.63	0.152%	0.52
	Moderate	0.67	0.63	0.189%	0.52
	Extensive	0.83	0.63	0.248%	0.52
D	Minor	0.29	0.65	0.189%	0.54
	Moderate	0.37	0.65	0.260%	0.54
	Extensive	0.51	0.65	0.381%	0.54

The effect of the site profile is considerably reduced when PGV/V_{s30} is used where the fragility curves for all site profiles fall within a relatively narrower band. This means that the variability of the fragility curve caused by the soil characteristics is reduced by including the soil parameter in the intensity measure. Table 2 describes the fragility function parameters for damage states of the tunnel using PGA and PGV/V_{s30}. The standard deviations of fragility curves in the case using PGV/V_{s30} are shown to be smaller than those using PGA, highlighting that the uncertainty in the fragility curve is reduced when using of PGV/V_{s30} as the intensity measure instead of PGA.

6 CONCLUDING REMARKS

A set of fragility curves of a double box cut-and-cover tunnel were developed using a series of pseudo-static analyses. Sixteen site profiles were considered for calculating horizontal soil displacement in 1D site response analysis. Fragility curves for three damage states were derived with respect to PGA and PGV/V_{s30}. The influence of site profile on the developed fragility curves was shown to be important. The site effects resulted in a wider distribution for the PGA based fragility curves compared with the PGV/V_{s30} based curves. The standard deviation of PGV/V_{s30} based fragility functions were smaller because the site stiffness is accounted for in addition to the intensity. It is thus demonstrated that PGV/V_{s30} is a better parameter to develop fragility curves of tunnels than PGA.

ACKNOWLEDGEMENT

This study was funded by the project titled "*Development of performance-based seismic design technologies for advancement in design codes for port structures*" (Ministry of Oceans and Fisheries of Korea) and Basic Science Research Program through the National Research Foundation of Korea (Ministry of Science, ICT and Future Planning, NRF-2015R1A2A2A01006129) a grant (18SCIP-B146946-01) from Construction technology research program funded by Ministry of Land, Infrastructure and Transport of Korean government.

REFERENCES

ALA, 2001. Seismic fragility formulations for water systems: Part 1-Guideline. American Society of Civil Engineers – FEMA.

Anderson, D.G., 2008. Seismic analysis and design of retaining walls, buried structures, slopes, and embankments. Transportation Research Board, USA.

Argyroudis, S., Kaynia, A.M., Pitilakis, K., 2013. Development of fragility functions for geotechnical constructions: application to cantilever retaining walls. Soil Dynamics and Earthquake Engineering 50, 106-116.

Argyroudis, S., Pitilakis, K., 2012. Seismic fragility curves of shallow tunnels in alluvial deposits. Soil Dynamics and Earthquake Engineering 35, 1-12.
Argyroudis, S., Tsinidis, G., Gatti, F., Pitilakis, K., 2017. Effects of SSI and lining corrosion on the seismic vulnerability of shallow circular tunnels. Soil Dynamics and Earthquake Engineering 98, 244-256.
CSI, 2011. SAP2000 software, ver15. Berkeley, California, USA.
Darendeli, M., 2001. Development of new family of normalized modulus reduction and material damping curves. University of Texas, Austin, USA.
Debiasi, E., Gajo, A., Zonta, D., 2013. On the seismic response of shallow-buried rectangular structures. Tunnelling and underground space technology 38, 99-113.
Dowding, C.H., Rozan, A., 1978. Damage to rock tunnels from earthquake shaking. Journal of the Soil Mechanics and Foundations Division 104, 175-191.
Hashash, Y., Karina, K., Koutsoftas, D., O'Riordan, N., 2010. Seismic design considerations for underground box structures, Earth Retention Conference, Washington, USA, pp. 620-637.
Hashash, Y., Musgrove, M., Harmon, J., Groholski, D., Phillips, C., Park, D., 2015. DEEPSOIL 6.0, User Manual, 114 p.
Hashash, Y.M., Hook, J.J., Schmidt, B., John, I., Yao, C., 2001. Seismic design and analysis of underground structures. Tunnelling and Underground Space Technology 16, 247-293.
HAZUS, 2004. Multi-hazard loss estimation methodology: Earthquake model, Department of Homeland Security, FEMA, Washington, DC, USA.
Hwang, J.-H., Lu, C.-C., 2007. Seismic capacity assessment of old Sanyi railway tunnels. Tunnelling and underground space technology 22, 433-449.
Iai, S., 2005. International Standard (ISO) on seismic actions for designing geotechnical works–an overview. Soil Dynamics and Earthquake Engineering 25, 605-615.
Iida, H., Hiroto, T., Yoshida, N., Iwafuji, M., 1996. Damage to Daikai subway station. Soils and foundations, 283-300.
Lee, T.H., Park, D., Nguyen, D.D., Park, J.S., 2016b. Damage analysis of cut-and-cover tunnel structures under seismic loading. Bulletin of Earthquake Engineering 14, 413-431.
Liu, T., Chen, Z., Yuan, Y., Shao, X., 2016. Fragility analysis of a subway station structure by incremental dynamic analysis. Advances in Structural Engineering, 1369433216671319.
MLTM, 2009. Earthquake resistance design regulations for subway structures. Ministry of Land, Transport and Maritime Affais of Korea.
Nguyen, D.D., Lee, T.H., Park, D., 2018. Seismic Damage Analysis of Box Metro Tunnels Accounting for Aspect Ratio and Shear Failure. Submitted to Geomechanics and Engineering.
Park, D., Sagong, M., Kwak, D.-Y., Jeong, C.-G., 2009. Simulation of tunnel response under spatially varying ground motion. Soil Dynamics and Earthquake Engineering 29, 1417-1424.
Penzien, J., 2000. Seismically induced racking of tunnel linings. Earthquake Engineering & Structural Dynamics 29, 683-691.
Qiu, W., Huang, G., Zhou, H., Xu, W., 2018. Seismic Vulnerability Analysis of Rock Mountain Tunnel. International Journal of Geomechanics 18, 04018002.
Salmon, M., Wang, J., Jones, D., Wu, C., 2003. Fragility formulations for the BART system, Advancing Mitigation Technologies and Disaster Response for Lifeline Systems. ASCE, Long Beach, Calif., USA, pp. 183-192.
Tang, W.H., Ang, A., 2007. Probability concepts in engineering: Emphasis on applications to civil & environmental engineering. Wiley Hoboken, NJ. USA.
Tsinidis, G., Rovithis, E., Pitilakis, K., Chazelas, J.L., 2016. Seismic response of box-type tunnels in soft soil: Experimental and numerical investigation. Tunnelling and Underground Space Technology 59, 199-214.
Wang, J.-N., 1993. Seismic design of tunnels: a simple state-of-the-art design approach. Parsons Brinckerhoff.
Wood, J.H., 2004. Earthquake design procedures for rectangular underground structures. Earthquake Commission Research Foundation.
Yoo, J.-K., Park, J.-S., Park, D., Lee, S.-W., 2017. Seismic response of circular tunnels in jointed rock. KSCE Journal of Civil Engineering, 1-9.
Zou, Y., Liu, H., Jing, L., Cui, J., 2017. A pseudo-static method for seismic responses of underground frame structures subjected to increasing excitations. Tunnelling and Underground Space Technology 65, 106-120.